Cell Reports, Volume *31*

Supplemental Information

Actin Assembly around the *Shigella*-Containing Vacuole Promotes Successful Infection

Sonja Kühn, John Bergqvist, Magdalena Gil, Camila Valenzuela, Laura Barrio, Stéphanie Lebreton, Chiara Zurzolo, and Jost Enninga

Inventory of Supplemental Information

SUPPLEMENTAL FIGURES

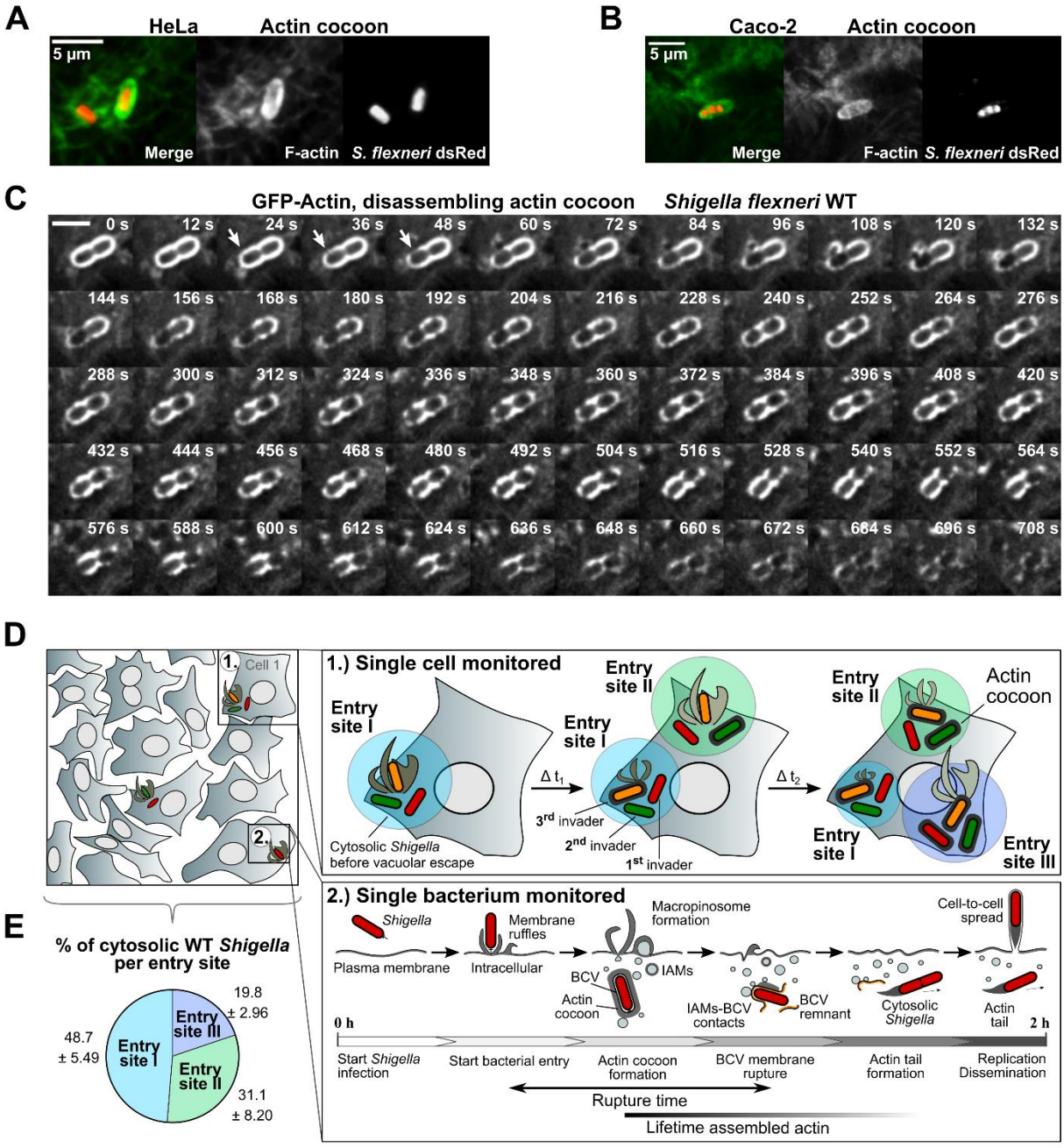

Figure S1. Actin cocoons contain F-actin and their formation depends on the order of infection, Related to Figure 1

(**A-B**) Immunofluorescence images of HeLa (A) and Caco-2 cells (B) expressing endogenous actin. Cells were infected with DsRed-expressing *Shigella* WT strain and phalloidin-labeled for F-actin (green). (**C**) Real-time images showing that actin cocoons disassemble simultaneously at different locations while undergoing constant reassembly during *Shigella* WT infection in actin-GFP expressing HeLa cells (scale bar: 3 μm). (**D**) Experimental setup to investigate successive invasion steps of *Shigella* in real time. Successive steps are monitored simultaneously at single cell (1) and single bacterium (2) levels. This allows correlating them within the cellular context and with other invading bacteria. In this setup (at MOI of 40; Figure S2), single cells were infected on average via three (3.03±0.46) distinct entry sites per cell (I, II, and III). The 1^{st} (red), 2^{nd} (green) and 3^{rd} (orange) invader of each entry site were considered in our analysis. (**E**) Almost half of the cytosolic *Shigella* WT entered host cells via the 1^{st} entry site, while about 1/3 bacteria invaded via the 2^{nd} and 1/5 via the 3^{rd} foci. (**F-G**) Rupture time (F) and actin cocoon assembly (G) depend on the entry site and order of infection. Depicted is the in-depth analysis of *Shigella* WT that developed an actin cocoon from Figure 1F, G (n=4, N=446). The rupture time of individual 1^{st}, 2^{nd}, or 3^{rd} bacteria invading the same cell through different entry sites is similar (F). The probability of actin cocoon formation for individual bacteria depends on the order of infection and the specific entry site (G). All late invading bacteria polymerize an actin cocoon. All 3^{rd} invaders of foci II and III in all independent experiments had an actin cocoon. Error bars indicate ± SD (F), Mann-Whitney test with $p<0.05$ as significant (*$p<0.05$, ns: not significant). In (E, G), mean values ± SD are indicated.

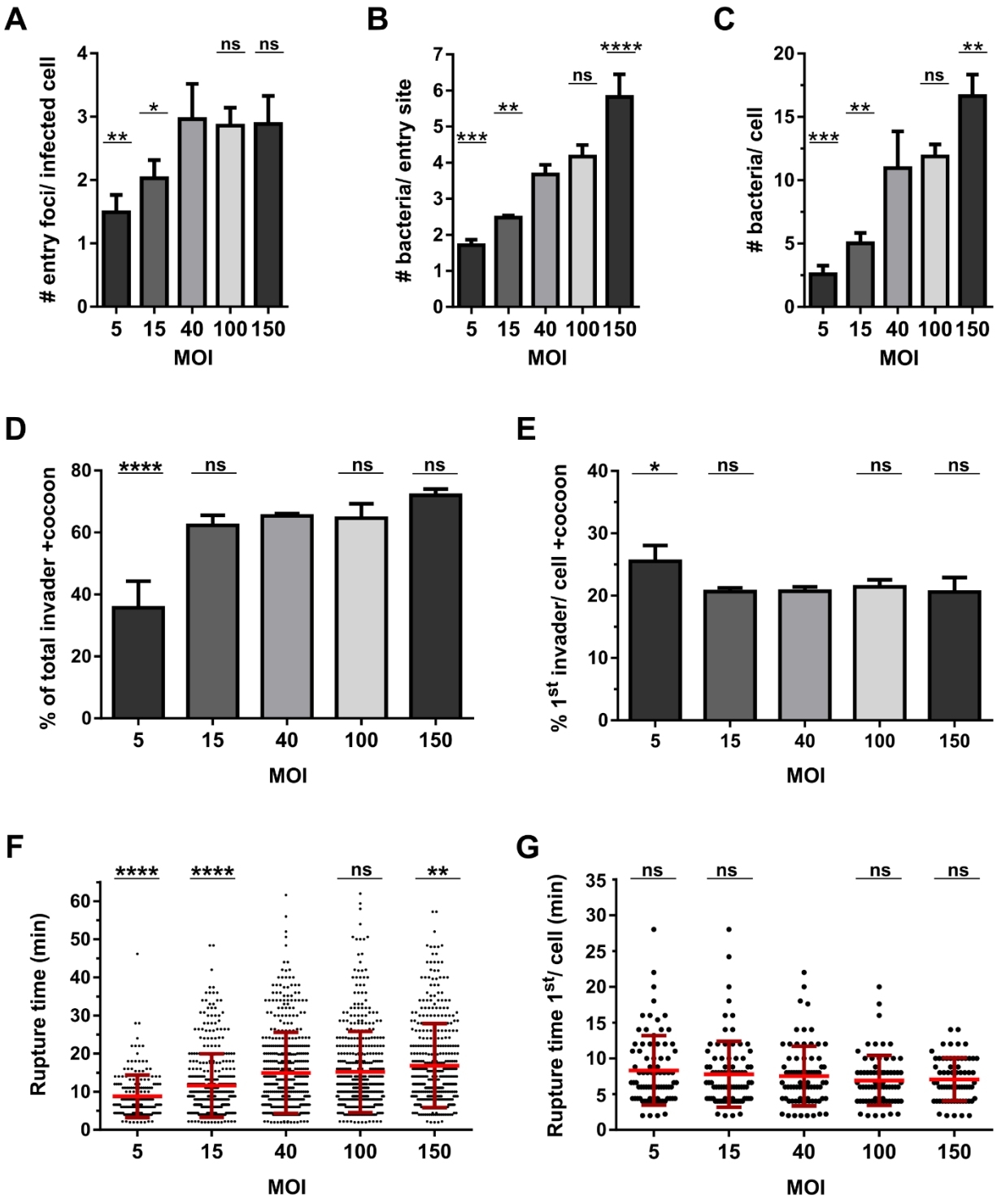
A
entry foci/ infected cell
MOI
B
bacteria/ entry site
MOI
C
bacteria/ cell
MOI
D
% of total invader +cocoon
MOI
E
% 1st invader/ cell +cocoon
MOI
F
Rupture time (min)
MOI
G
Rupture time 1st/ cell (min)
MOI

Figure S2. The multiplicity of infection (MOI) defines the number of entering *Shigella* per individual cell, but not the probability of actin cocoon formation, Related to Figure 1

The effect of MOIs from 5 to 150 was investigated with regards to entry sites per infected cell (**A**), successfully invading bacteria per entry site (**B**), overall number of invading bacteria per cell (**C**), the probability of cocoon formation (**D-E**) and vacuolar escape time (**F-G**). The higher the MOI, the more bacteria enter via the same entry site. The quickly saturated effect of the MOI to cocoon formation (D) and rupture time (F) is likely caused by the increased probability for cocoon assembly of later entering bacteria (Figure S1). Since with high MOI more bacteria per entry site invade host cells, there are more late invaders present that assemble an actin cocoon. This probably increases the percentage of the total cytosolic *Shigella* with cocoons at higher MOIs compared to very low ones. Comparing the same bacterial population, here the 1st invading *Shigella* per cell, leads to no difference in actin cocoon formation and vacuolar escape (E, G). In (A-D, F), total invading *Shigella* populations were analyzed (n=3, N=2000 bacteria with MOI 5: 203, MOI 15: 430, MOI 40: 477, MOI 100: 461, MOI 150: 429)). In (E, G), only the 1st invaders per cell of the same experiments were taken into account (N=385 with MOI 5: 81, MOI 15: 86, MOI 40: 78, MOI 100: 72, MOI 150: 68). Mean values ± SD are indicated as error bars. Statistical significance was determined using one-way ANOVA or Student's *t*-test comparing individual MOI experiments with MOI 40. $p<0.05$ was considered as significant (*$p<0.05$, **$p<0.01$, ***$p<0.001$, ****$p<0.0001$, ns: not significant).

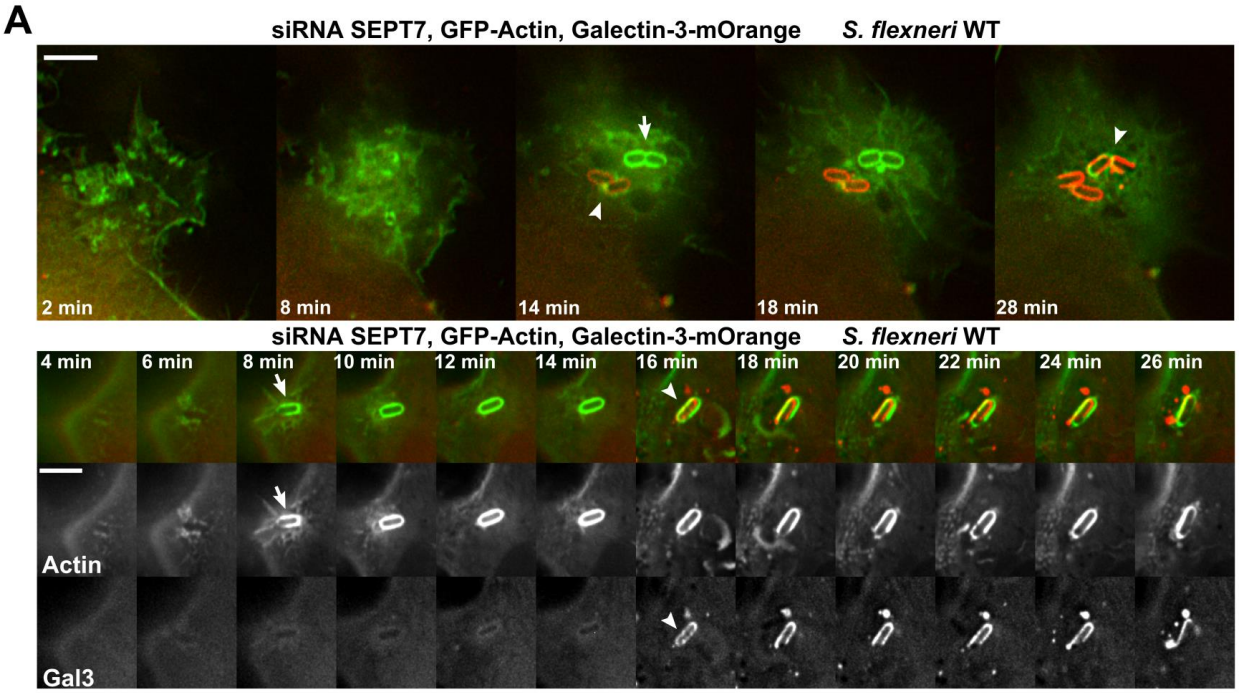
A
siRNA SEPT7, GFP-Actin, Galectin-3-mOrange
S. flexneri WT
2 min
8 min
14 min
18 min
28 min
siRNA SEPT7, GFP-Actin, Galectin-3-mOrange
S. flexneri WT
4 min
6 min
8 min
10 min
12 min
14 min
16 min
18 min
20 min
22 min
24 min
26 min
Actin
Gal3

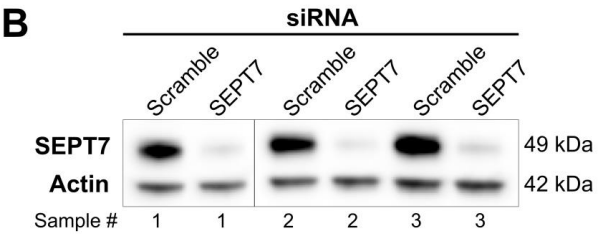
B
siRNA
Scramble
SEPT7
SEPT7
Actin
49 kDa
42 kDa
Sample #
1 1 2 2 3 3

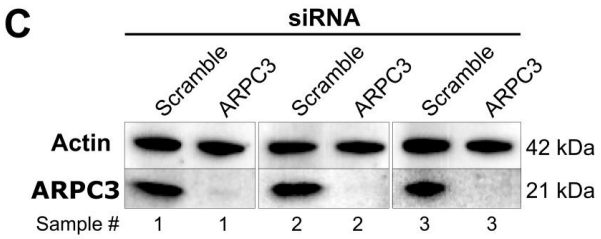
C
siRNA
Scramble
ARPC3
Actin
ARPC3
42 kDa
21 kDa
Sample #
1 1 2 2 3 3

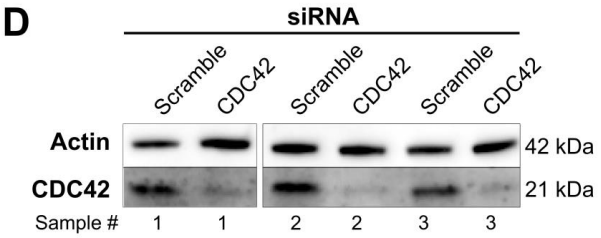
D
siRNA
Scramble
CDC42
Actin
CDC42
42 kDa
21 kDa
Sample #
1 1 2 2 3 3

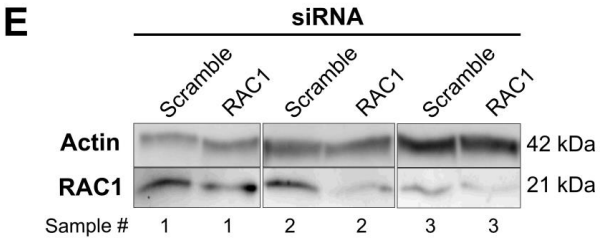
E
siRNA
Scramble
RAC1
Actin
RAC1
42 kDa
21 kDa
Sample #
1 1 2 2 3 3

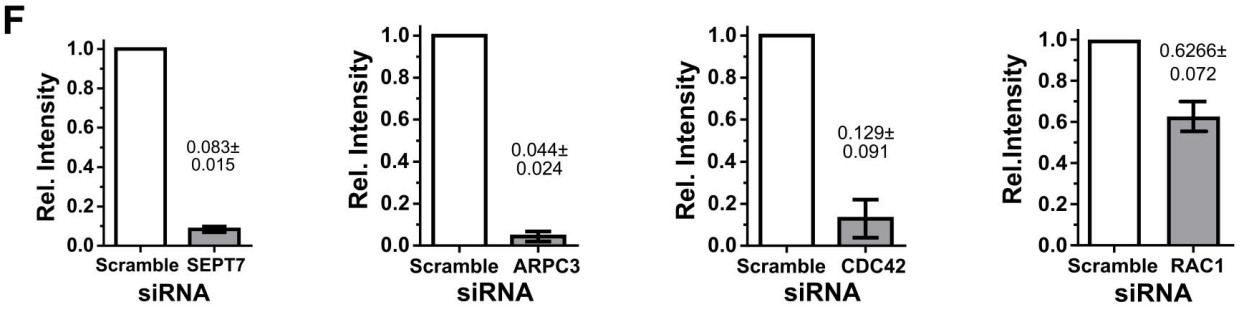
F
Rel. Intensity
0.083± 0.015
Scramble SEPT7
siRNA
0.044± 0.024
Scramble ARPC3
siRNA
0.129± 0.091
Scramble CDC42
siRNA
0.6266± 0.072
Rel.Intensity
Scramble RAC1
siRNA

Figure S3. Characterization of the actin cocoon and the tools for its analysis, Related to Figure 2, 4 and 6

(**A**) Septin 7 knockdown does not prevent actin cocoon assembly. Representative time-lapses of HeLa cells treated with SEPTIN 7 (SEPT7) siRNA and co-transfected with actin and galectin-3. Upper panel: entry site during *Shigella* WT infection, lower panel: actin cocoon dynamics and successive infection steps during invasion of an individual *Shigella* bacterium. t=0 min: start entry site formation, arrow: start cocoon assembly, arrow head: BCV rupture, scale bar: 5 µm. (**B-E**) Western blot validation of siRNA treatments against SEPT7 (B), the Arp2/3 complex component ARPC3 (C), CDC42 (D) and RAC1 (E). Samples of n=3 independent experiments are shown compared to scramble siRNA control. (**F**) Quantification of unmodified images revealed knockdown (KD) efficiencies of 91.7% (SEPT7, A), 95.6% (ARPC3, B), 87.1% (CDC42, C) and 37,3% (RAC1, D). Of note, CDC42 knockdown, although less efficient, had a stronger effect on cocoon assembly than ARPC3 knockdown. This could indicate other CDC42 functions in cocoon formation beside Arp2/3 complex activation. The contrast in the figures was enhanced to highlight KD efficiency.

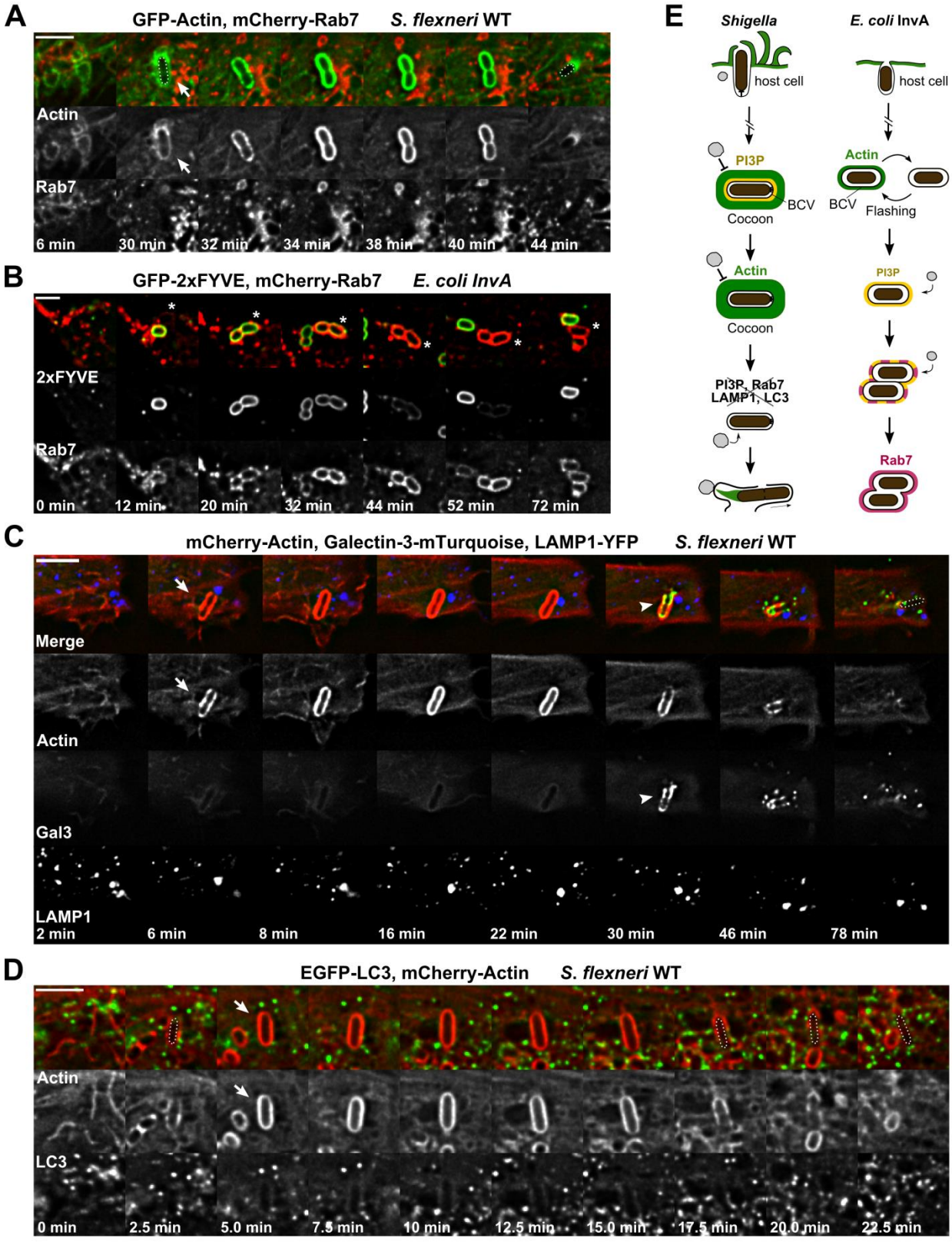
A
GFP-Actin, mCherry-Rab7
S. flexneri WT
Actin
Rab7
6 min
30 min
32 min
34 min
38 min
40 min
44 min
B
GFP-2xFYVE, mCherry-Rab7
E. coli InvA
2xFYVE
Rab7
0 min
12 min
20 min
32 min
44 min
52 min
72 min
E
Shigella
E. coli InvA
host cell
host cell
PI3P
BCV
Cocoon
Actin
BCV
Flashing
Actin
Cocoon
PI3P
PI3P, Rab7
LAMP1, LC3
Rab7
C
mCherry-Actin, Galectin-3-mTurquoise, LAMP1-YFP
S. flexneri WT
Merge
Actin
Gal3
LAMP1
2 min
6 min
8 min
16 min
22 min
30 min
46 min
78 min
D
EGFP-LC3, mCherry-Actin
S. flexneri WT
Actin
LC3
0 min
2.5 min
5.0 min
7.5 min
10 min
12.5 min
15.0 min
17.5 min
20.0 min
22.5 min

Figure S4. Markers for canonical endosomal maturation and autophagy are not recruited to the *Shigella* BCV surrounded by the actin cocoon, Related to Figure 2

(**A**) Representative time-lapse monitoring Rab7 localization during *Shigella* WT infection. (**B**) Time-lapse imaging showing the maturation of *E. coli* InvA phagosomes and recruitment of Rab7 after the initial PI3P peak. (**C-D**) Time-lapse imaging of LAMP1 (C) and LC3 (D) localization during *Shigella* WT infection indicates no recruitment to the BCV. For *Shigella*, HeLa cells were co-transfected with the corresponding fluorescent marker protein and actin to monitor the successive infection steps from membrane ruffle to actin tail formation. All bacteria were moving inside the cell in the last shown image, indicating cytosolic bacteria that successfully escaped the BCV. t=0 min: start entry site formation, arrow: start cocoon assembly, arrow head: BCV membrane rupture indicated by galectin-3 recruitment, scale bars: 5 μm (A, C-D), 3 μm (B). Selected *Shigella* WT and *E. coli InvA* bacteria are highlighted with dashed lines and stars, respectively. (**E**) Model illustrating the localization of autophagy and maturation markers at the *Shigella* BCV and the *E. coli* InvA phagosome. The *Shigella* BCV exhibits an altered maturation process after rapid depletion of PI3P leading to rupture with intracellular replication and dissemination. This is different to canonical phagosomes: After actin flashing, the phagosome becomes PI3P positive followed by Rab7 recruitment and PI3P depletion for vesicle fusion events with vacuolar maturation and degradation.

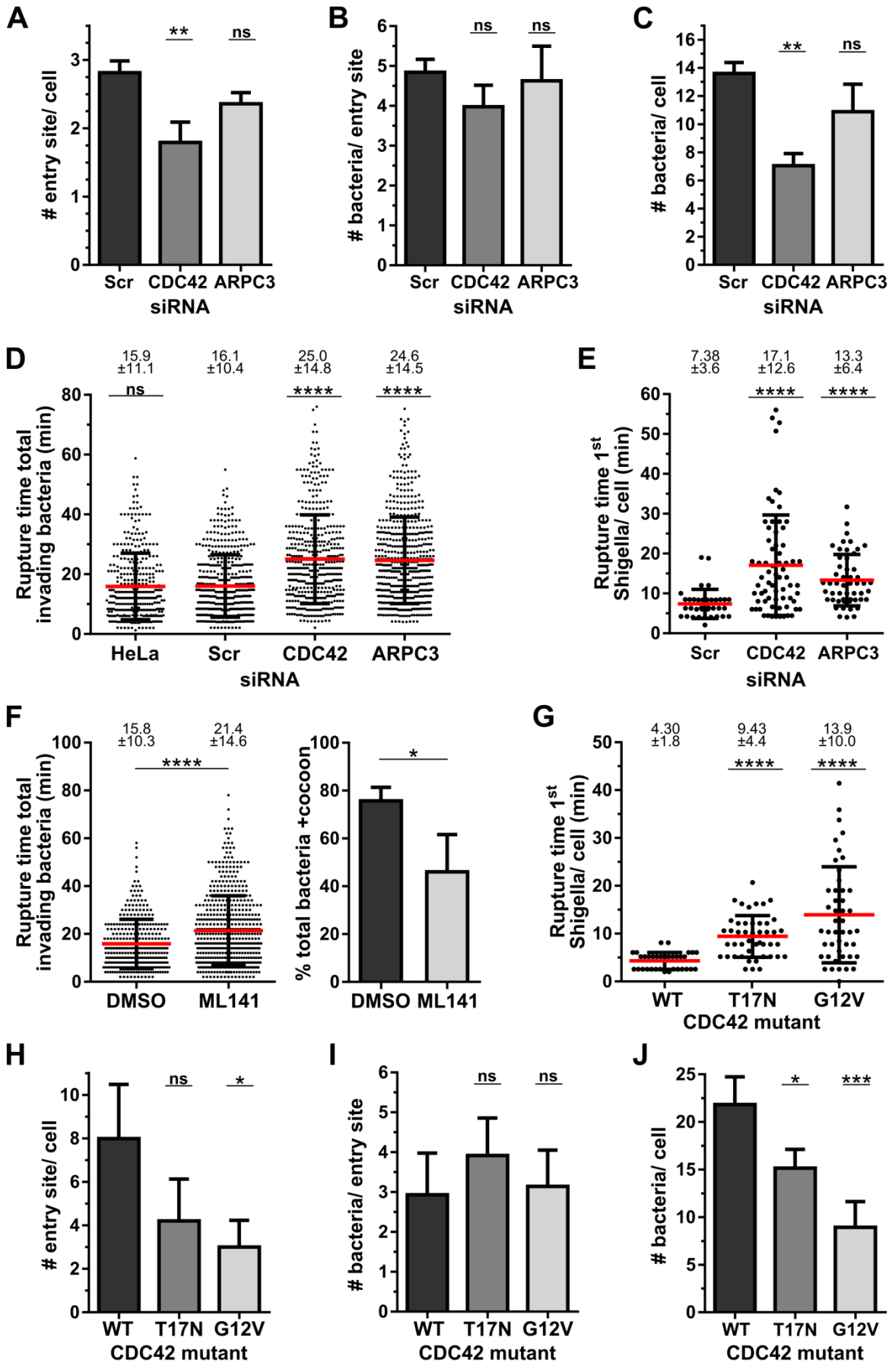
A
entry site/ cell
**
ns
Scr
CDC42
ARPC3
siRNA
B
bacteria/ entry site
ns
ns
Scr
CDC42
ARPC3
siRNA
C
bacteria/ cell
**
ns
Scr
CDC42
ARPC3
siRNA
D
15.9 ±11.1
16.1 ±10.4
25.0 ±14.8
24.6 ±14.5
ns
****
****
Rupture time total invading bacteria (min)
HeLa
Scr
CDC42
ARPC3
siRNA
E
7.38 ±3.6
17.1 ±12.6
13.3 ±6.4
****
****
Rupture time 1st Shigella/ cell (min)
Scr
CDC42
ARPC3
siRNA
F
15.8 ±10.3
21.4 ±14.6
****
Rupture time total invading bacteria (min)
DMSO
ML141
*
% total bacteria +cocoon
DMSO
ML141
G
4.30 ±1.8
9.43 ±4.4
13.9 ±10.0
****
****
Rupture time 1st Shigella/ cell (min)
WT
T17N
G12V
CDC42 mutant
H
ns
*
entry site/ cell
WT
T17N
G12V
CDC42 mutant
I
ns
ns
bacteria/ entry site
WT
T17N
G12V
CDC42 mutant
J
*
***
bacteria/ cell
WT
T17N
G12V
CDC42 mutant

Figure S5. CDC42 and the Arp2/3 complex are involved in host cell invasion, Related to Figure 4
Depicted are additional statistics for the experiments shown in Figure 4. Only bacteria that successfully escaped into the host cytosol were considered for quantitative analysis. (**A-E**) Knockdown of CDC42 and ARPC3. Decreased cellular levels of CDC42 lowered the number of entry sites per infected cell (A) and thus the number of invading bacteria per cell (C). Decreased levels of CDC42 and ARPC3 delayed the rupture times for all invading bacteria per experiment (D) and the first invaders per cell (E). Knockdown efficiency was confirmed by immunoblotting (Figure S3). (**F**) Inhibition of CDC42 with the inhibitor ML141 increases the rupture time (left) and impairs cocoon assembly (right) around vacuolar *Shigella*. (**G-J**) HeLa cells co-expressing galectin-3 and CDC42 WT, T17N or G12V were infected with *Shigella* WT. Presented are the rupture time of the first invading *Shigella* per cell (G), number of entry sites per cell (H), number of bacteria per entry site (I), and total number of invading bacteria per cell (J). Depicted are error bars indicating ± SD, or mean values ± SD. One-way ANOVA or Student's *t*-test was used to determine significance compared to infected Scr or DMSO control or to CDC42 WT-expressing cells. $p<0.05$ was considered as significant (*$p<0.05$, **$p<0.01$, ***$p<0.001$, ****$p<0.0001$, ns: not significant). Counted events: (A-D) no siRNA (HeLa): N=374, control scramble siRNA (Scr): N=481, siRNA CDC42: N=464, siRNA ARPC3: N=573; (E) Scr siRNA: N=36, siRNA CDC42: N=69, siRNA ARPC3: N=52; (F) DMSO (control): N=341, ML141: N=553; (G): WT: N=34, T17N: N=47, G12V: N=47; (H-J): WT: N=373, N=T17N: N=375, G12V: N=375.

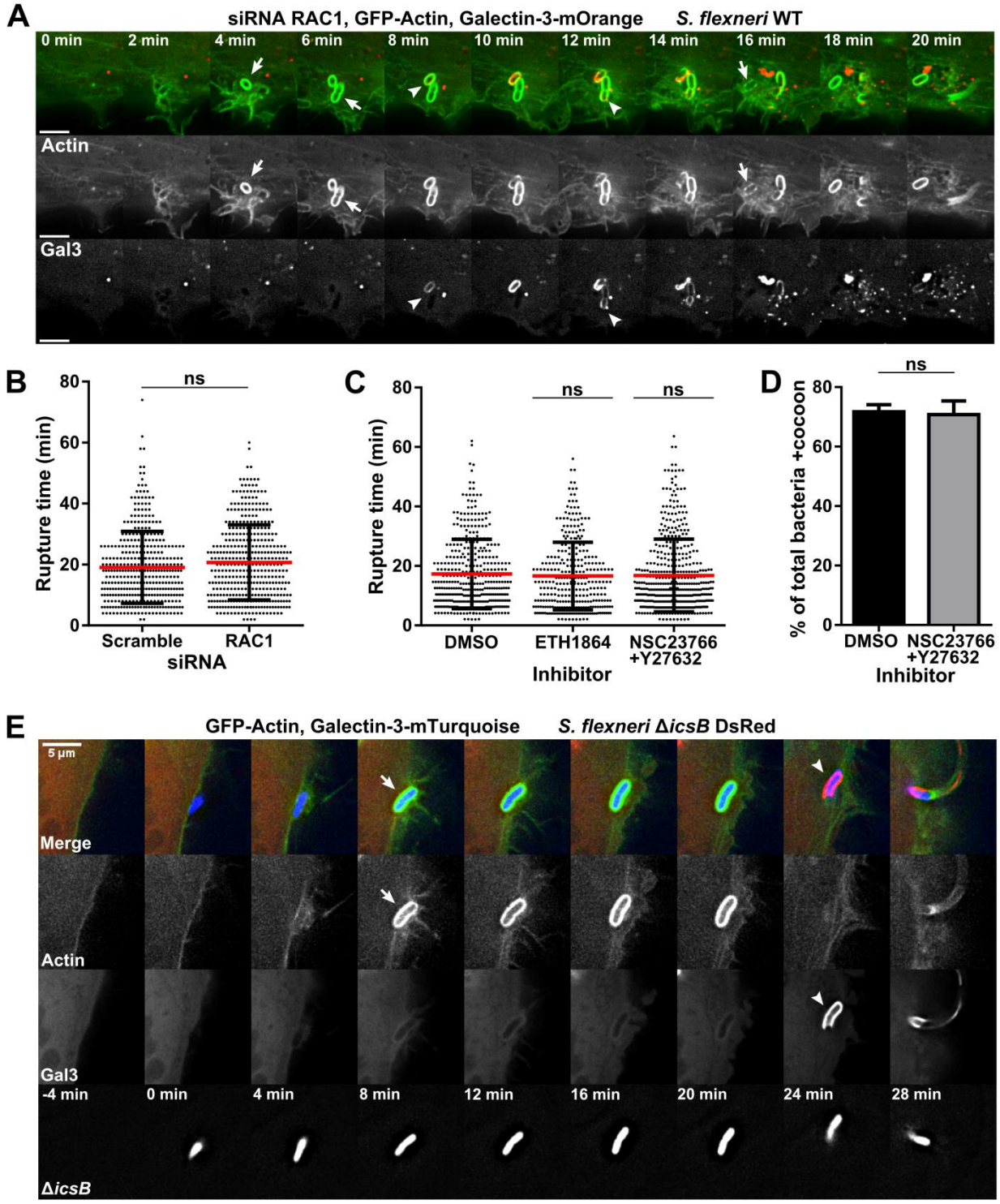
A
siRNA RAC1, GFP-Actin, Galectin-3-mOrange
S. flexneri WT
0 min
2 min
4 min
6 min
8 min
10 min
12 min
14 min
16 min
18 min
20 min
Actin
Gal3
B
Rupture time (min)
ns
Scramble
RAC1
siRNA
C
Rupture time (min)
ns
ns
DMSO
ETH1864
NSC23766 +Y27632
Inhibitor
D
% of total bacteria +cocoon
ns
DMSO
NSC23766 +Y27632
Inhibitor
E
GFP-Actin, Galectin-3-mTurquoise
S. flexneri ΔicsB DsRed
5 µm
Merge
Actin
Gal3
-4 min
0 min
4 min
8 min
12 min
16 min
20 min
24 min
28 min
ΔicsB

Figure S6. RAC1 is not required for actin cocoon assembly, Related to Figure 4 and 5

(**A-B**) Representative time-lapse (A) and quantification (B) of the experiment shown in Figure 4F. RAC1 knockdown does neither prevent actin cocoon assembly, nor affect the rupture time of invading *Shigella* WT. RAC1 siRNA treated HeLa cells were co-transfected with actin and galectin-3. (**C-D**) Small molecule inhibition of RAC1 (ETH1864, NSC23766) and ROCK (Y27632) did not interfere with the rupture time (C) or cocoon assembly (D). Error bars ± SD or mean values ± SD are illustrated, ns: not significant. Counted events: (B) scramble siRNA: N=386, siRNA RAC1: N=409; (C-D) DMSO: N=385, ETH1864: N=328, NCS23766+Y21632: N=464. (**E**) Representative time-lapse of HeLa cells co-transfected with actin and galectin-3 and infected with DsRed-expressing *Shigella* Δ*icsB*. t=0 min: start entry site formation, arrow: start cocoon assembly, arrow head: BCV membrane rupture, scale bars: 5 μm.

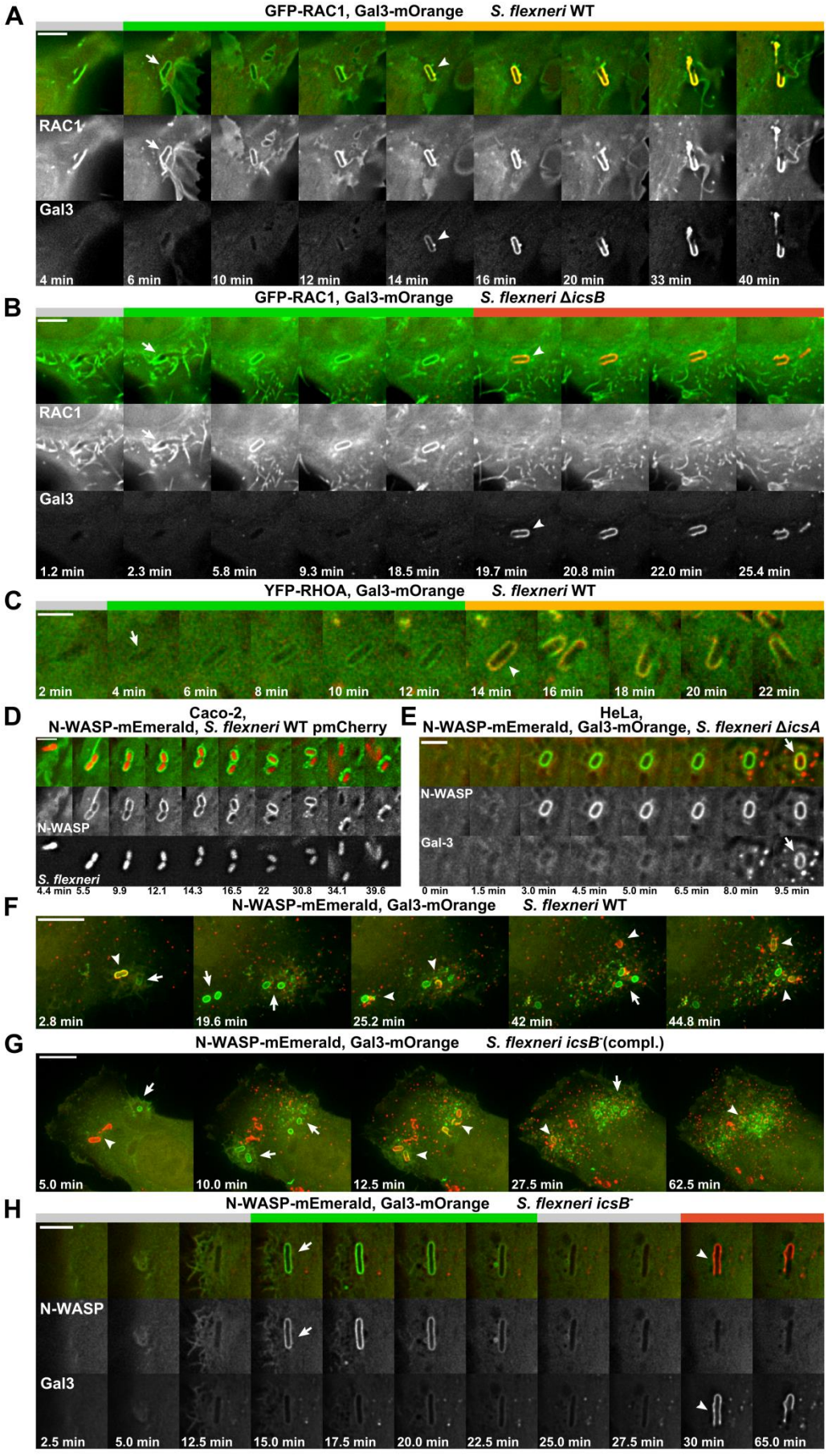
A
GFP-RAC1, Gal3-mOrange S. flexneri WT
RAC1
Gal3
4 min
6 min
10 min
12 min
14 min
16 min
20 min
33 min
40 min
B
GFP-RAC1, Gal3-mOrange S. flexneri ΔicsB
RAC1
Gal3
1.2 min
2.3 min
5.8 min
9.3 min
18.5 min
19.7 min
20.8 min
22.0 min
25.4 min
C
YFP-RHOA, Gal3-mOrange S. flexneri WT
2 min
4 min
6 min
8 min
10 min
12 min
14 min
16 min
18 min
20 min
22 min
D
Caco-2,
N-WASP-mEmerald, S. flexneri WT pmCherry
N-WASP
S. flexneri
4.4 min 5.5
9.9
12.1
14.3
16.5
22
30.8
34.1
39.6
E
HeLa,
N-WASP-mEmerald, Gal3-mOrange, S. flexneri ΔicsA
N-WASP
Gal-3
0 min
1.5 min
3.0 min
4.5 min
5.0 min
6.5 min
8.0 min
9.5 min
F
N-WASP-mEmerald, Gal3-mOrange S. flexneri WT
2.8 min
19.6 min
25.2 min
42 min
44.8 min
G
N-WASP-mEmerald, Gal3-mOrange S. flexneri icsB-(compl.)
5.0 min
10.0 min
12.5 min
27.5 min
62.5 min
H
N-WASP-mEmerald, Gal3-mOrange S. flexneri icsB-
N-WASP
Gal3
2.5 min
5.0 min
12.5 min
15.0 min
17.5 min
20.0 min
22.5 min
25.0 min
27.5 min
30 min
65.0 min

Figure S7. Rho GTPase and N-WASP recruitment to the BCV, Related to Figure 6

(**A-B**) RAC1 is recruited to most BCVs and localizes constantly around the *Shigella*-containing vacuole dependent on IcsB, like CDC42. Depicted are representative time-lapses of HeLa cells co-transfected with RAC1 and galectin-3 (Gal3) (scale bars: 5 μm). (**C**) Most bacteria do not recruit RHOA at their BCV. The time lapse shows an example of this occasional event in HeLa cells (22% of cytosolic bacteria; scale: 3 μm). (**D**) As in HeLa cells, N-WASP is likewise constantly localized around the BCV of mCherry-expressing *S. flexneri* WT (red) invading Caco-2 cells transiently expressing N-WASP (scale: 3 μm). (**E**) Constant N-WASP localization at the BCV is IcsA-independent. A representative time-lapse of HeLa cells co-transfected with N-WASP and galectin-3 and infected with *Shigella* Δ*icsA* is shown (scale: 3 μm). Initial N-WASP recruitment before vacuolar rupture and its constant localization are similar to WT infections (see Figure 6). (**F-H**) N-WASP is constantly localized at BCVs of WT (F) or IcsB-complemented *icsB*$^{-}$ (compl.) (G) strains (3.5 μm stacks of infection sites, scale bars: 10 μm). *Shigella icsB*$^{-}$ initially recruits N-WASP at its BCV, but does not cluster it there in the moment of vacuolar rupture (H, scale bar: 5 μm). *Shigella* strains in (F-H) were poly-L-lysine-coated. t=0 min: start entry, arrow: start cocoon, arrow head: BCV membrane rupture.